Enhanced transport in the polar mesosphere of Jupiter: Evidence from Cassini UVIS helium 584 Å airglow

C. D. Parkinson,[1,2] A. I. F. Stewart,[3] A. S. Wong,[4] Y. L. Yung,[1] and J. M. Ajello[5]

Received 26 July 2005; accepted 16 September 2005; published 11 February 2006.

[1] The eddy diffusion profile (K) in the auroral regions of Jupiter is not well determined. However, because of the intense auroral energy input, eddy mixing is expected to be much more effective and may be responsible for the enhancement of heavy hydrocarbon production in the polar region. In this paper, we estimate the increased eddy mixing in the Jovian auroral regions by comparing the Cassini Ultraviolet Imaging Spectrograph (UVIS) observations during the 2000 Jupiter flyby with radiative transfer calculations of the He 584 Å airglow intensity. We derive a range for the eddy diffusion coefficients at the homopause (K_h) in the auroral regions to be at least 8×10^6 cm^2 s^{-1} and possibly greater than 4×10^7 cm^2 s^{-1}. By comparison, equatorial K_h is on the order of 2×10^6 cm^2 s^{-1}.

Citation: Parkinson, C. D., A. I. F. Stewart, A. S. Wong, Y. L. Yung, and J. M. Ajello (2006), Enhanced transport in the polar mesosphere of Jupiter: Evidence from Cassini UVIS helium 584 Å airglow, *J. Geophys. Res.*, *111*, E02002, doi:10.1029/2005JE002539.

1. Introduction

[2] One of the fundamental properties of a planetary atmosphere is the amount of mechanical mixing forced by the large-scale circulation, planetary and gravity waves, and other processes. In a one-dimensional model, this mixing is often characterized by the eddy diffusion profile, K. At the homopause, the altitude where the molecular diffusion coefficient equals the eddy diffusion coefficient, we define $K = K_h$. Values of K_h for Jupiter have been obtained from analyses of (1) the H Lyman alpha albedo [*Wallace and Hunten*, 1973; *Yung and Strobel*, 1980; *Gladstone et al.*, 1996], (2) the falloff in hydrocarbon profiles against H_2 background, using the Voyager Ultraviolet Spectrometer (UVS) occultation results for the CH_4 and other hydrocarbon distributions [*Festou et al.*, 1981; *Yelle et al.*, 1996], and (3) the He 584 Å airglow [*McConnell et al.*, 1981; *Vervack et al.*, 1995]. Analysis of the equatorial He 584 Å emission data suggests values of K_h in the range 10^6–10^7 cm^2 s^{-1} [*McConnell et al.*, 1981] and 2 (+2, −1) $\times 10^6$ cm^2 s^{-1} [*Vervack et al.*, 1995], in reasonable agreement with those values obtained by methods 1 and 2. Since for an ionospheric source of H the column amount above the absorbing layer of methane decreases monotonically with increasing eddy diffusion coefficient, K, the measured Lyman α brightness could yield an estimate of the K. Determining K_h using this method is strictly valid only if (1) resonance scattering alone is responsible for the observed Lyman α emission, (2) H is produced only from the photochemical processes involving H_2, CH_4, etc., and (3) the solar Lyman α flux is known accurately [*Atreya*, 1986]. However, the status of our knowledge of the Lyman α budget for Jupiter is uncertain and other sources of excitation may play a role [*McConnell et al.*, 1989; *Clarke et al.*, 1991; *Ben Jaffel et al.*, 1993]. Moreover, issues regarding the solar Lyman α flux have always been a problem [*Parkinson et al.*, 1998]. Hence stellar occultation and He 584 Å airglow may be the best way to determine a "reasonably" secure value for K.

[3] The eddy diffusion coefficient in the auroral regions of Jupiter is poorly known. However, because of the intense auroral energy input, eddy mixing is expected to be much more effective and hence may be responsible for the enhancement of heavy hydrocarbon production in the polar regions [*Wong et al.*, 2003]. A crude estimate of K can be made on the basis of mixing length theory *Lindzen* [1971]. K can be expressed as $K \sim vL$, where v = velocity of two air parcels that interchange and mix thoroughly with the background over distance L [*Atreya*, 1986, p. 68]. In auroral regions, with additional energy input from the magnetosphere, we speculate that it is not unreasonable to expect both v and L to increase relative to equatorial regions and hence K to be greater in the polar regions.

[4] Recent observations by the Cassini Ultraviolet Imaging Spectrograph (UVIS) of the Jovian He 584 Å emission allow a derivation of a range of K in the polar regions. In this paper, we investigate evidence for increased eddy

[1]Division of Geological and Planetary Sciences, California Institute of Technology, Pasadena, California, USA.
[2]Jet Propulsion Laboratory and NASA Astrobiology Institute, Pasadena, California, USA.
[3]Laboratory for Atmospheric and Space Physics, University of Colorado, Boulder, Colorado, USA.
[4]Department of Atmospheric, Oceanic, and Space Sciences, University of Michigan, Ann Arbor, Michigan, USA.
[5]Jet Propulsion Laboratory, Pasadena, California, USA.

0148-0227/06/2005JE002539

mixing in the auroral regions of Jupiter by calculating the range of K_h from the UVIS data and employing new model atmospheres and radiative transfer models.

2. Observations

[5] The Cassini UVIS [*Esposito et al.*, 1998, 2004] observed the Jovian system during the Jupiter flyby from 1 October 2000 through 22 March 2001 during a period of near solar maximum activity. Two data sets containing the HeI 584 Å emissions are analyzed here, the first representing about 2×10^6 s of long-range (1190–585 Jovian radii (R_J)) data at poor spatial resolution (1.2–0.6 R_J) and the second containing more than 5 hours of observations from 245 R_J with a spatial resolution of 0.25 R_J.

[6] For 45 days, 1 October through 14 November 2000, observations were made in a mode that imaged the Jovian system on UVIS's 2-D CODACON detectors, with spatial resolution of 1 mrad and spectral resolution of about 3 Å. Details regarding the UVIS instrument construction and calibration are contained in work by *Esposito et al.* [1998, 2004]. The range to Jupiter decreased from 1170 to 618 R_J; Jupiter's phase decreased from 20° to 18°; the subspacecraft latitude remained between 3°N and 4°N. The spectral range of UVIS's EUV spectrometer is 569–1190 Å, and Jupiter's image at 584 Å was well separated both from its auroral and airglow H_2 emissions (850 Å and higher) and from the emissions from Io's plasma torus at 642 Å, 659 Å, and longer wavelengths. Over the 45 days, 2000 images, each with an integration period of 1000 s, were obtained covering 7 out of every 12 Jovian rotations. This is equivalent to 23 days of continuous observation.

[7] Because of the considerable range to Jupiter in this data set, the planet's disc was barely resolved. The following analysis deals only with the total photon flux from the entire disc (i.e., mean brightness, disc averaged). The images analyzed here were added together in groups of 29–36 (i.e., covering approximately 1 Jovian rotation) to improve the signal to noise. After subtracting a considerable instrument background and then scaling to a standard range of 1000 R_J, the 62 such groups yielded on average about 460 counts, with a RMS deviation of about 135 counts. Using the instrument sensitivity at 584 Å, the count rate was converted to the equivalent brightness of a uniformly emitting flat disk having the same diameter as the planet. The brightnesses thus obtained averaged 8.7 Rayleighs (R), with an RMS deviation of 1.8 R and a range of 5–15 R. Typical subsolar brightnesses for Voyager and Extreme Ultraviolet Explorer (EUVE) were ~4 R and 1.3 ± 0.5 R, respectively [*McConnell et al.*, 1981; *Gladstone and Hall*, 1998].

[8] The image count rates converted to Rayleighs at 584 Å are shown as the data points and solid line in the top plot of Figure 1. The squares and dashed line in the bottom plot of Figure 1 are the auroral signal due to H_2 emissions, normalized to the He I emissions. The two prominent spikes in the longer-wavelength signal coincide with the arrival at Jupiter of strong solar wind shocks [*Gurnett et al.*, 2002]. We also see from Figure 1 that the trend in the helium airglow emission is decreasing during the time of ingress from 1200 to 600 Jovian radii, whereas the Jovian auroral signal shows a lesser decrease. We interpret this to mean the whole system is cooling off during these 45 days (the signals from the Io torus also declined [*Steffl et al.*, 2004]). If the auroral input to the atmosphere declines, and if less energy means less vertical mixing, then one would expect the He 584 Å signal to decline also. From an initial qualitative inspection, it seems that the airglow and auroral signals might appear correlated, but analysis showed the correlation coefficients are too small to indicate a strong connection. The implication of a small correlation coefficient is that it indicates that the auroral zone contribution to the 584 Å signal is not large.

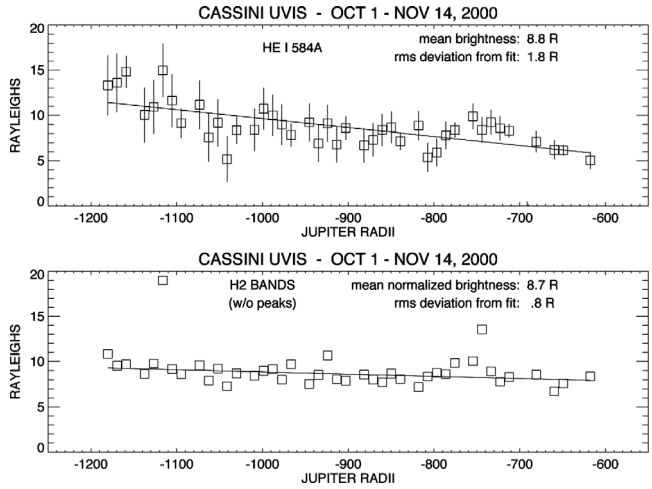

Figure 1. Disc-averaged HeI 584 Å brightnesses compared to the auroral signal (normalized) for the period 1 October to 14 November 2000. The plotted points represent the average signal during 42 complete or almost complete Jovian rotations. The error bars on the 584 Å points are the 1-sigma statistical uncertainties; the equivalent uncertainties in the auroral points are smaller than the symbols. The average of the 584 Å points is 8.7 ± 1.8 R, and they correlate with the auroral signal with a coefficient of 0.58. The two high auroral points correspond to the passage of large solar wind shocks.

[9] On 14 December 2000, Jupiter was at zero phase, at a range of 245 R_J. UVIS observed Jupiter for a total of about 5.4 hours. The line of sight was fixed on the planet's center, and the slit was parallel to its rotation axis. The EUV channel had 8 pixels placed along the subspacecraft meridian. For this data set, the north and south auroral zones and the nonauroral airglow are all clearly separable. Since the planet was viewed through the intervening Io plasma torus, the polar and equatorial spectra obtained also contain the torus's ionic emissions. This is more evident at wavelengths near 584 Å, where the planet itself is black (except for the helium feature), than at wavelengths longward of 850 Å, where the planet emits copiously from its aurorae and airglow.

[10] Figure 2 shows the EUV spectrum of Jupiter accumulated over 24,420 s on 14–15 December 2000, at a distance of 246 Jovian radii (17.6 million km) from the planet. Note the change in scale near 870Å by a factor of 10. Several emissions from Io's plasma torus are indicated. The H_2 emissions (in the Lyman and Werner band systems)

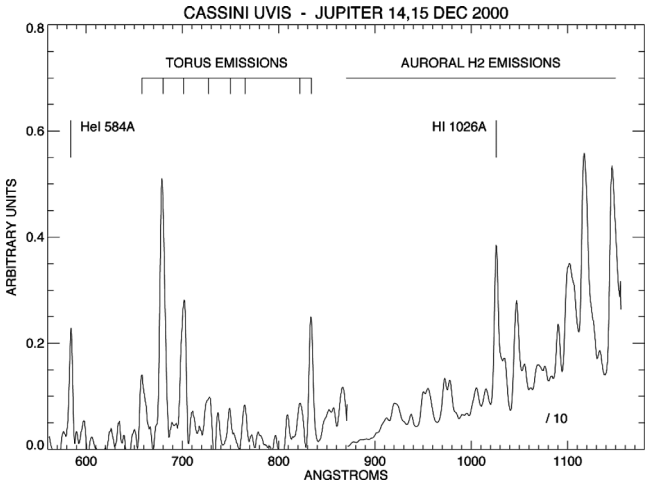

Figure 2. EUV spectrum of Jupiter accumulated over 24,420 s on 14–15 December 2000, at a distance of 246 R_J (17.6 million km) from the planet. Note the change in scale near 870 Å. Several emissions from Io's plasma torus are indicated, specifically, S II, S III, and S IV.

come predominantly from the auroral zones. In this wavelength range the auroral and airglow spectra are very similar; they both arise from electron impact on H_2. It should be remembered that the auroral zones themselves are not resolved; rather the auroral spectrum represents all the photons emitted at high latitudes, whether from the narrow auroral zones or from the airglow beyond about 60°N or 45°S.

[11] Figure 3 shows the north-south profile of the HeI 584A emission, measured on 14–15 December 2000 at a spatial resolution of 0.25 R_J. In Figure 3, increasing detector row corresponds to a south to north direction. The image of the planet fell on rows 25–38 of the UVIS 2-D CODACON detector. The UVIS high-resolution (2.4 Å) slit was parallel to, and centered on, the Jovian spin axis. The average brightness along the slit was 6.4 R, with a signal-to-noise ratio of 6.7. Background signals of 3.5 R due to radioactive thermal generator (RTG) gamma rays and of 9.4 R due to a light leak that admitted interplanetary Lyman α. The background (scattered light and RTG gamma-ray noise) level is shown, as is an empirical model of the 584 Å airglow signal, which varies as the cosine of latitude and peaks at 9.2 R. The bottom plot of Figure 3 shows the deduced excess signal that can be attributed to auroral processes. Also shown is the auroral signal normalized to the excess 584 Å signal. The apparent equatorward displacement of the 584 Å signal from the northern auroral signal is likely due to some combination of the greater depth of penetration of the auroral particles (resulting in more complete extinction of the emergent 584 Å signal), the possible dynamical transport of helium away from the aurora, and greater effective vertical mixing (higher homopause) equatorward of the north auroral zone. The error bars show the statistical uncertainties in the raw signals and in the excess signal obtained by subtraction of the background and airglow signals from the raw total. The solid line shows the He 584 Å signal. Also shown as a dashed line is the normalized auroral signal. We note that several more data sets taken close to the planet were obtained, but we defer their analysis to a later paper.

3. Model Description

[12] Resonance scattering of sunlight by He atoms is the principal source of the planetary emission at 584 Å [e.g., *Carlson and Judge*, 1974, 1976]. Since He is heavier than the background H_2 atmosphere, its mixing ratio falls off rapidly above the homopause. This results in the He being immersed in and overlaid by an absorbing atmosphere of H_2. The scattering region, that is, the region where the absorption optical depth in H_2 at 584 Å is less than 1, generally lies well above the homopause. As K_h increases, more He is mixed into the scattering region, and thus the reflected He 584 Å intensity increases.

[13] The principal parameters involved in determining the He 584 Å emission are f_{He}, the He volume mixing ratio well below the homopause, the solar He 584 Å flux and line shape, the atmospheric temperature profile, and the eddy diffusion coefficient profile. In our model we use f_{He} = 0.136 [*Niemann et al.*, 1996; *von Zahn and Hunten*, 1996]. The line-integrated solar flux at 1 AU is 4×10^9 cm^2 s^{-1}, corresponding to solar maximum conditions. A Gaussian line shape with a 1/*e* half width of 73 mÅ (or 122 mÅ FWHM) [*Maloy et al.*, 1978; *McConnell et al.*, 1981] is used and is compatible with the analyses of *Chassefiere et al.* [1988], *Bush and Chakrabarti* [1995], and *Krasnopolsky and Gladstone* [1996]. The reader is referred to *Parkinson et al.* [1998] for a comprehensive discussion regarding He 584 Å solar flux and line shape. We apply a resonance

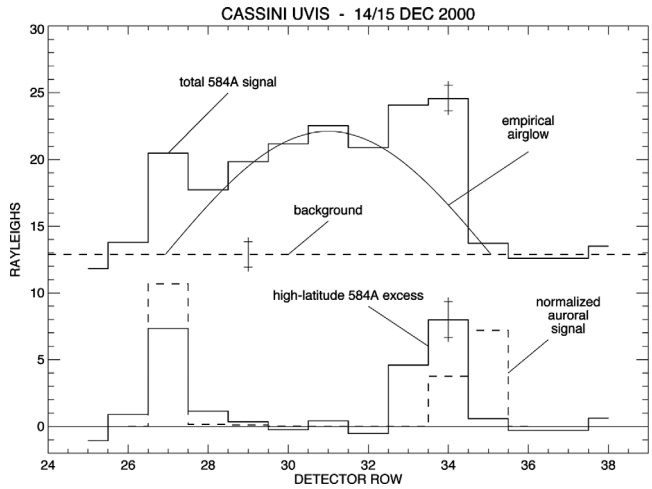

Figure 3. (top) North-south profile of the HeI 584 Å emission, measured on 14–15 December 2000 at a spatial resolution of 0.25 R_J. In our case, increasing detector row corresponds to a south to north direction. The background (scattered light and RTG gamma-ray noise) level is shown, as is an empirical model of the 584 Å airglow signal, which varies as the cosine of latitude and peaks at 9.2 R. (bottom) Deduced excess signal which can be attributed to auroral processes. Also shown is the auroral signal normalized to the excess 584 Å signal. The error bars show the statistical uncertainties in the raw signals and in the excess signal obtained by subtraction of the background and airglow signals from the raw total.

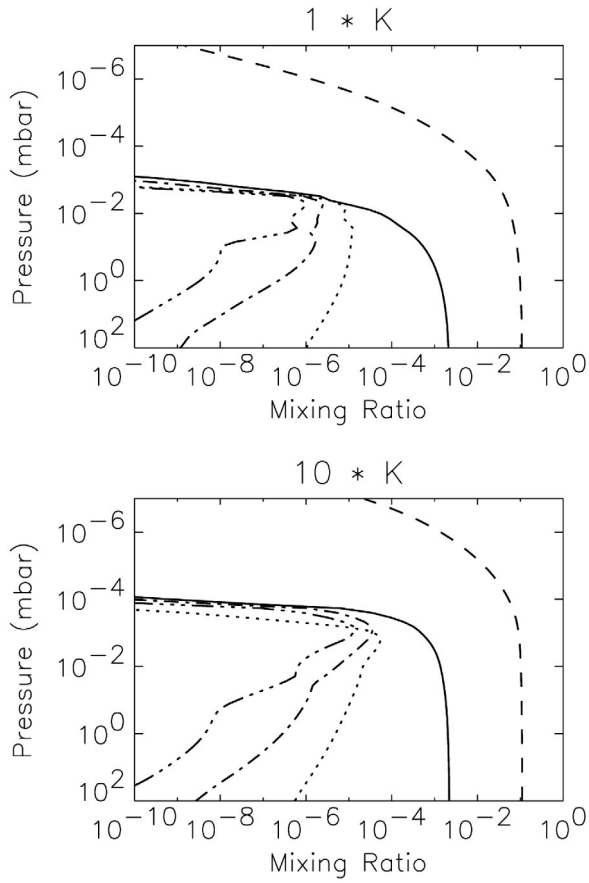

Figure 4. Mixing ratios of He (dashed line), CH_4 (solid line), C_2H_2 (dash-dotted line), C_2H_4 (dash-triple-dotted line), and C_2H_6 (dotted line) for eddy diffusion enhancement factor κ of 1 and 10 versus pressure, calculated using a Jovian polar chemical model at latitudes of 65°.

scattering model that uses the Feautrier technique to solve the equation of radiative transfer assuming partial frequency redistribution [*Gladstone*, 1982].

[14] The H_2 and He densities used in the resonance scattering model are calculated by a one-dimensional photochemical model for the polar atmosphere of Jupiter [see *Wong et al.*, 2003]. For our case, we consider the solar zenith angle to be equal to the viewing angle equal to the latitude to match the geometry of the observations. Both neutral and ion reactions are included in the photochemical model. The temperature profile and the auroral ion production rates are taken from the Jovian auroral thermal model of *Grodent et al.* [2001] in which the energy flux is 30.5 ergs cm^{-2} s^{-1}. They use a nominal value for K_h of 1.4×10^6 cm^2 s^{-1}. The molecular diffusion coefficients, D, used in our calculations are taken from *Mason and Marrero* [1970], *Atreya* [1986], and *Cravens* [1987]. K is adjustable in this study. For a nominal K, we use the expression similar to one suggested by *Atreya et al.* [1981] and *Gladstone et al.* [1996]:

$$K\left(\mathrm{cm^2 s^{-1}}\right) = \left(1.46 \times 10^6\right) \times \left(1.4 \times 10^{13}/n_t(z)\right)^{0.65}$$

above 100 mbar level and

$$K\left(\mathrm{cm^2 s^{-1}}\right) = 10^3$$

below 100 mbar, where $n_t(z)$ is the total number density at altitude z. We consider three cases of enhanced eddy diffusion profiles, given by κK, where κ = 1, 3, and 10. The homopause pressure level and K_h for each κ are (1.2×10^{-3} mbar, 9×10^5 cm^2 s^{-1}), (3.0×10^{-4} mbar, 9×10^6 cm^2 s^{-1}), and (2.6×10^{-5} mbar, 2×10^8 cm^2 s^{-1}), respectively. In each case, we generate the corresponding density profiles for background gases for each of the polar latitudes of 60°, 65°, and 70°. Figure 4 shows the calculated density profiles of key species at 65° with κ = 1 and 10. As expected, for models with higher κ, the mixing ratios of He and all hydrocarbons increase significantly above the homopause. Indeed, *Wong et al.* [2003] have found that a κ of ~15 is necessary to match the production of benzene and hydrocarbon aerosols with relevant observations [see *Wong et al.*, 2003, and references therein].

4. Results and Discussion

[15] From Figures 2 and 3, we see that there is evidence for high-latitude nonsolar sources of He 584Å emissions. These very interesting observations suggest that (1) electron impact is important, or (2) the atmosphere is horizontally/vertically inhomogeneous, or (3) both.

[16] Figure 5 shows a plot of auroral volume emission rate versus altitude for He 584 Å. The peak intensity of the emission layer occurs at 1400 km with a layer width of about 400 km. Integrated over the secondary electron distribution, the electron flux is 3×10^9 cm^{-2} s^{-1} at 1400 km and the He 584 Å emission cross section at 200 eV is 8×10^{-18} cm^{-2} [*Shemansky et al.*, 1985]. *Grodent et al.* [2001] (Figure 1) gives the He, atomic H and H_2 altitude profile. The helium number density is 10^4 cm^{-3} at 1400 km with a corresponding column density of 10^{11} cm^{-2}. The helium is excited by the primary electron flux [cf. *Grodent et al.*, 2001, section 3] which is composed of a superposition of three Maxwellians: a hard flux at 15 keV with peak deposition at 250 km; a soft flux at 3 keV with

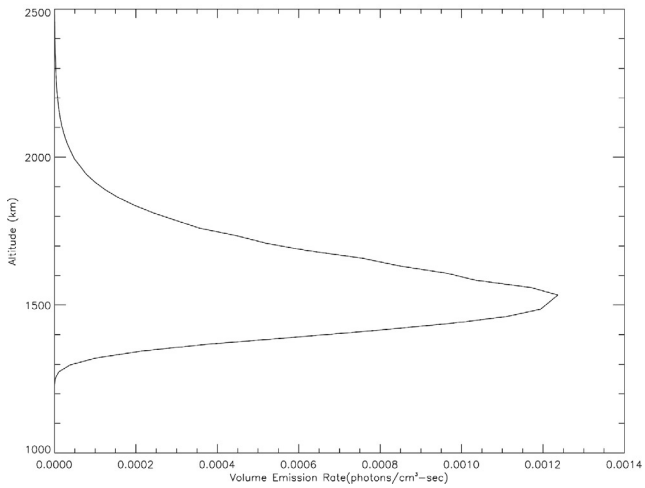

Figure 5. He 584 Å auroral volume emission rate as a function of altitude. The peak intensity of the emission layer occurs at 1400 km (~2×10^{-7} mbars) with a layer width of about 400 km corresponding to an integrated value of less than 0.1 R.

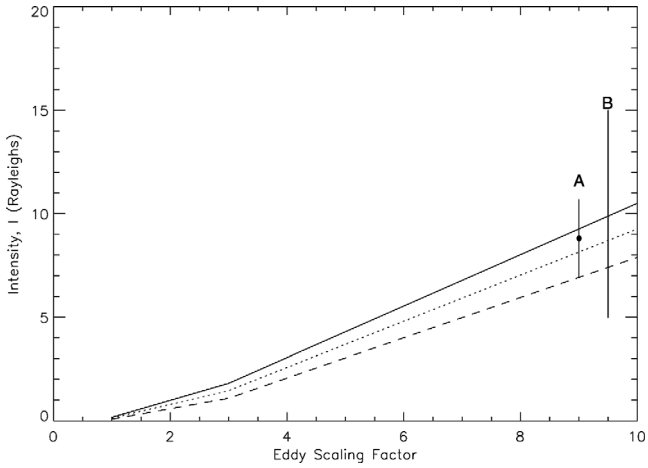

Figure 6. Calculated He 584 Å emission intensity on Jupiter as a function of κ for different latitudes. The calculations are for the case where solar zenith angle equals the viewing angle equals latitude using the standard temperature profile, standard value for f_{He}, and the model atmosphere generated using the standard eddy diffusion profile. On the right-hand side of the diagram, we show the range of emergent He 584 Å intensities taken from the Cassini/UVIS experiment observations: "A" represents the average of the 584 Å points of 8.7 ± 1.8 R as shown in Figure 1, and "B" represents the raw range of values from 5 to 15 R. Here the various curves are 60° (solid curve), 65° (dotted curve), and 70° (dashed curve).

peak deposition at 600 km; and a weak flux at 100 eV with peak deposition at about 1500 km [see *Grodent et al.*, 2001, Figure 6]. The absolute electron fluxes that *Grodent et al.* [2001] give agree within a factor of about 2 with that needed to model the observed intensities of the H_2 aurora from Cassini. These weak and soft primary electrons will produce the high-altitude He aurora that would emerge from the planet to be observed by Cassini if it is there. The cross section and the energy flux from *Grodent et al.* [2001] allow the calculation of the *g* factor (the electron excitation rate, s^{-1}) for either the weak (100 eV) or soft (3 keV) primary flux and the *Grodent et al.* [2001] model He, atomic H and H_2 atmosphere give the volume emission rate and the attenuation to the top of the atmosphere. Using the *Grodent et al.* [2001] model atmosphere, we estimate the column emission intensity of He 584 Å due to electron precipitation to be negligible at about 0.01 R, thus eliminating point 1 as a possible emission source. While this He brightness depends on the temperature and *K*, we did not perform a sensitivity study here since the value we obtained was so low that even a 2 order of magnitude increase would still only be ~1 R. Additionally, we have used typical values corresponding to those of *Grodent et al.* [2001]. They do consider a case of 10 times the nominal value for *K*, but only for H_3^+ and not He.

[17] If the atmosphere's vertical/horizontal inhomogeneity is the main cause, it could be due to enhanced eddy diffusion coefficients allowing more helium to be mixed into the scattering region. However, other mechanisms should also be considered. Auroral input can deposit energy into a specific altitude region such that this region heats up, the atmosphere expands, and winds are generated. For instance, *Liu and Dalgarno* [1996] report that large temperature gradients occur with respect to altitude within the Jovian auroral emission regions. Also, *Raynaud et al.* [2004] reanalyze the 1971 Beta Scorpii occultation data by the south polar region of Jupiter, showing that characteristics of the temperature gradient and the spectral behavior of the temperature fluctuations are in agreement with the presence of atmospheric propagating gravity waves in the Jovian atmosphere. This might allow species like helium to be carried to a higher-altitude region with a larger scale height and a more extensive He distribution, but the same happens to H_2, which acts as a shielding gas, and would be consistent with their results, which correspond to a value of $K_h = 2 \times 10^6$ cm^2 s^{-1}. From these analyses, we conclude that temperature fluctuations cannot be considered as a possible source of atmospheric inhomogeneity.

[18] *Drossart et al.* [2000] generate a vertical profile of helium using a diffusion equation, with a fixed value of $K_h = 1.5 \times 10^6$ cm^2 s^{-1}, providing evidence that the CH_4 homopause level on Jupiter does not vary much across the disk. However, the assumption of an a priori value for K_h leaves their analysis ambiguous regarding atmospheric inhomogeneity. Also, this value is much lower than calculated values retrieved from methane fluorescence at 3.3 μm observed from ISO/SWS [*Drossart et al.*, 1999]. If confirmed by further analysis, this difference could be due to a spatial variability of the eddy diffusion coefficient on Jupiter.

[19] In Figure 6 we compare the calculated He 584 Å emission intensities for various values of κ with measured intensity. The calculated He 584 Å intensity is plotted as a function of κ for latitudes 60°, 65°, and 70°. The intensity increases with decreasing latitude, showing some He 584 Å dependence on differences in solar zenith angle. The UVIS He 584 Å measurement range is shown in Figure 6. When comparing the model results with the measurement using Figure 6, one can determine the possible range for κ. For example, κ at 60°, 65°, and 75° have lower bounds of about 5.5, 6, and 7, respectively, and in all cases, an upper bound greater than 10 in order to reproduce the observed He 584 Å emission intensity in the range of 5–15 R (range B). If we consider the value of 8.7 R ± 1.8 R (range A), the lower bound is even higher with a minimum enhancement factor ranging between 7 and 9. The results derived from the present study for He 584 Å airglow are consistent with that of the previous chemical study for aerosol production [*Wong et al.*, 2003]. It is also seen in Figure 6 that the He 584 Å brightness is very low for small values of κ when compared to equatorial model atmospheric brightness calculations, where we expect values close to the Voyager helium airglow analysis of *McConnell et al.* [1981]. This is mainly due to a greatly enhanced atomic hydrogen column of about a factor of 50 in the upper mesosphere for the polar model atmosphere (in which there is enhanced dissociation of H_2 and CH_4) we are using over standard equatorial model atmospheres previously used.

[20] A significant shortcoming of the UVIS data lies in its limited spatial resolution, which results in narrow arcs of auroral emissions and diffuse polar airglow emissions appearing in the same pixel or pixels. Other uncertainties arise from the lack of actual measurements of the auroral energy deposition profile. Additionally, there is a disparity

between the Voyager and Cassini epoch He 584Å airglow values. The present estimates of the subsolar equatorial He 584Å value (8.7 R) exceed those of Voyager by a factor of about 2. Calibration uncertainties in both instruments may contribute to this, but the secular change in Figure 1 implies that natural He 584 Å brightness variations are possible. We are aware of these problems and defer discussion of these them until a full analysis of the entire data set collected is done. Despite this, our investigation shows mechanical mixing in the polar mesosphere of Jupiter is in the range of 4 to more than 10 times of the nominal eddy mixing profile K. Thus our modeling indicates that the observed high-latitude He emissions are consistent with enhanced eddy diffusion coefficients in the Jovian auroral regions. Additional observations are needed to confirm this conjecture. More realistic modeling than a simple 1-D model with eddy diffusion is required. We hope this work provides further motivation for the continuing development of 2-D and 3-D models for the upper atmosphere of Jupiter and other giant planets.

[21] **Acknowledgments.** This work was supported by NASA grant NAG5-6263 and the National Aeronautics and Space Administration through the NASA Astrobiology Institute under cooperative agreement CAN-00-OSS-01 issued through the Office of Space Science. A.I.F.S. acknowledges support from the National Aeronautics and Space Administration through JPL contract 961196 and also the great and successful efforts of the UVIS team. A.S.W. thanks Sushil Atreya for discussion and valuable comments. The authors thank editor Julie Moses and reviewers Jack McConnell and Mike Summers for their thorough and thoughtful review and comments.

References

Atreya, S. K. (1986), *Atmospheres and Ionospheres of the Outer Planets and Their Satellites*, Springer, New York.

Atreya, S. K., T. M. Donahue, and M. C. Festou (1981), Jupiter: Structure and composition of the upper atmosphere (theory), *Astrophys. J.*, *247*, L43–L47.

Ben Jaffel, L., J. T. Clarke, R. Prangé, G. R. Gladstone, and A. Vidal-Madjar (1993), The Lyman alpha bulge of Jupiter: Effects of non-thermal velocity field, *Geophys. Res. Lett.*, *20*, 747–750.

Bush, B. C., and S. Chakrabarti (1995), Analysis of Lyman α and He I 584-Å airglow measurements using a spherical radiative transfer model, *J. Geophys. Res.*, *100*, 19,609–19,625.

Carlson, R. W., and D. L. Judge (1974), Pioneer 10 ultraviolet photometer observations at Jupiter encounter, *J. Geophys. Res.*, *79*, 3623–3633.

Carlson, R. W., and D. L. Judge (1976), Pioneer 10 ultraviolet photometer observations at Jupiter: The helium to hydrogen ratio, in *Jupiter*, edited by T. Gehrels, pp. 418–440, Univ. of Ariz. Press, Tucson.

Chassefiere, E., F. Dalaudier, and J.-L. Bertaux (1988), Estimate of interstellar helium parameters from Prognoz 6 and Voyager 1/2: EUV resonance glow measurements taking into account a possible redshift in the solar line profile, *Astron. Astrophys.*, *210*, 113–122.

Clarke, J. T., G. R. Gladstone, and L. Ben Jaffel (1991), Jupiter's dayglow H Ly-α emission line profile, *Geophys. Res. Lett.*, *18*, 1935–1938.

Cravens, T. E. (1987), Vibrationally excited molecular hydrogen in the upper atmosphere of Jupiter, *J. Geophys. Res.*, *92*, 11,083–11,100.

Drossart, P., T. Fouchet, J. Crovisier, E. Lellouch, T. Encrenaz, H. Feuchtgruber, and J. P. Champion (1999), Flourescence in the 3 micron bands of methane on Jupiter and Saturn from ISO/SWS observations, in *The Universe As Seen by ISO*, edited by P. Cox and M. F. Kessler, *Eur. Space Agency Spec. Publ.*, *ESA SP-427*, 169–172.

Drossart, P., B. Sicardy, F. Roques, T. Widemann, G. R. Gladstone, J. H. Waite, and M. Vincent (2000), The methane homopause of Jupiter as seen in IR spectroscopy from the occultation of star HIP9369, *Bull. Am. Astron. Soc.*, *32*, 1013.

Esposito, L. W., J. E. Colwell, and W. E. McClintock (1998), Cassini UVIS observations of Saturn's rings, *Planet. Space Sci.*, *46*, 1221–1235.

Esposito, L. W., et al. (2004), The Cassini ultraviolet imaging spectrograph investigation, *Space Sci. Rev.*, *115*, 299–361.

Festou, M. C., S. K. Atreya, T. M. Donahue, B. R. Sandel, D. E. Shemansky, and A. L. Broadfoot (1981), Composition and thermal profiles of the Jovian upper atmosphere determined by the Voyager Ultraviolet Stellar Occultation experiment, *J. Geophys. Res.*, *86*, 5715–5725.

Gladstone, G. R. (1982), Radiative transfer with partial frequency redistribution in inhomogeneous atmospheres: Application to the Jovian aurora, *J. Quant. Spectrosc. Radiat. Transfer*, *27*, 545–556.

Gladstone, G. R., and D. T. Hall (1998), Recent results from EUVE observations of the Io plasma torus and Jupiter, *J. Geophys. Res.*, *103*, 19,927–19,933.

Gladstone, G. R., M. Allen, and Y. L. Yung (1996), Hydrocarbon photochemistry in the upper atmosphere of Jupiter, *Icarus*, *119*, 1–52.

Grodent, D., J. H. Waite Jr., and J.-C. Gerard (2001), A self-consistent model of the Jovian auroral thermal structure, *J. Geophys. Res.*, *106*, 12,933–12,952.

Gurnett, D. A., et al. (2002), Control of Jupiter's radio emission and aurorae by the solar wind, *Nature*, *415*, 985–987.

Krasnopolsky, V. A., and G. R. Gladstone (1996), Helium on Mars: EUVE and PHOBOS data and implications for Mars' evolution, *J. Geophys. Res.*, *101*, 15,765–15,772.

Lindzen, R. S. (1971), Tides and gravity in the upper atmosphere, in *Mesospheric Models and Related Experiments*, edited by G. Fiocco, pp. 122–130, Springer, New York.

Liu, W., and A. Dalgarno (1996), The ultraviolet spectra of the Jovian aurora, *Astrophys. J.*, *467*, 446–453.

Maloy, J. O., R. W. Carlson, U. G. Hartmann, and D. L. Judge (1978), Measurement of the profile and intensity of the solar He I λ584 Å resonance line, *J. Geophys. Res.*, *83*, 5685–5690.

Mason, E. A., and T. R. Marrero (1970), The diffusion of atoms and molecules, in *Advances in Atomic and Molecular Physics*, vol. 6, edited by D. R. Bates and I. Esterman, pp. 155–232, Elsevier, New York.

McConnell, J. C., B. R. Sandel, and A. L. Broadfoot (1981), Voyager UV spectrometer observations of the He 584 Å dayglow at Jupiter, *Planet. Space Sci.*, *29*, 283–292.

McConnell, J. C., C. D. Parkinson, L. Ben-Jaffel, C. Emerich, R. Prangé, and A. Vidal-Madjar (1989), H Lyman α emission at Neptune: Voyager prediction, *Astron. Astrophys.*, *225*, L9–L12.

Niemann, H. B., et al. (1996), The Galileo probe mass spectrometer: Composition of Jupiter's atmosphere, *Science*, *272*, 849–851.

Parkinson, C. D., E. Griffioen, J. C. McConnell, G. R. Gladstone, and B. R. Sandel (1998), He 584 Å dayglow at Saturn: A reassessment, *Icarus*, *133*, 210–220.

Raynaud, E., K. Matcheva, P. Drossart, F. Roques, and B. Sicardy (2004), A re-analysis of the 1971 Beta Scorpii occultation by Jupiter: Study of temperature fluctuations and detection of wave activity, *Icarus*, *168*, 324–335.

Shemansky, D. E., J. M. Ajello, D. T. Hall, and B. Franklin (1985), Vacuum ultraviolet studies of electron impact of helium: Excitation of He (n1Po) Rydberg series and ionization excitation of He+ (nR) Rydberg series, *Astrophys. J.*, *296*, 774–783.

Steffl, A. J., A. I. F. Stewart, and F. Bagenal (2004), Cassini UVIS observations of the Io plasma torus. I. Initial results, *Icarus*, *172*, 78–90.

Vervack, R. J., B. R. Sandel, G. R. Gladstone, J. C. McConnell, and C. D. Parkinson (1995), A re-evaluation of the Jovian He 584 Å emissions, *Icarus*, *114*, 163–173.

von Zahn, U., and D. M. Hunten (1996), The helium mass fraction in Jupiter's atmosphere, *Science*, *272*, 849–851.

Wallace, L., and D. M. Hunten (1973), The Lyman-alpha albedo of Jupiter, *Astrophys. J.*, *182*, 1013–1031.

Wong, A. S., Y. L. Yung, and A. J. Friedson (2003), Benzene and haze formation in the polar atmosphere of Jupiter, Geophys. Res. Lett., *30(8)*, 1447, doi:10.1029/2002GL016661.

Yelle, R., L. A. Young, R. J. Vervack Jr., R. Young, L. Pfister, and B. R. Sandel (1996), Structure of Jupiter's upper atmosphere: Predictions for Galileo, *J. Geophys. Res.*, *101*, 2149–2161.

Yung, Y. L., and D. F. Strobel (1980), Hydrocarbon photochemistry and Lyman alpha albedo of Jupiter, *Astrophys. J.*, *239*, 395–402.

J. M. Ajello, Jet Propulsion Laboratory, MS 183-601, Pasadena, CA 91109, USA.

C. D. Parkinson and Y. L. Yung, Division of Geological and Planetary Sciences, California Institute of Technology 150-21, Pasadena, CA 91125, USA. (cdp@gps.caltech.edu)

A. I. F. Stewart, Laboratory for Atmospheric and Space Physics, University of Colorado, 1234 Innovation Drive, Boulder, CO 80309, USA.

A. S. Wong, Department of Atmospheric, Oceanic, and Space Sciences, University of Michigan, Ann Arbor, MI 48109-2143, USA.